Magazine of Civil Engineering

ISSN 2712-8172

journal homepage: http://engstroy.spbstu.ru/

DOI: 10.34910/MCE.110.2

Impact of elevated temperature on the shear behavior of strengthened RC beams

R. Al-Rousan

Jordan University of Science and Technology, Irbid, Jordan

E-mail: rzalrousan@just.edu.jo

Keywords: reinforced concrete, elevated temperature, shear strength, fiber reinforced polymer, experimental

Abstract. When the concrete structures are exposed to escalated temperatures (500°C and higher), concrete fails because of the decay of cement hydration products, development of vapor pressure, and undesired variations in the volume of ingredients. Heat-damaged concrete structures can restore their strength when strengthened with carbon fiber-reinforced polymer (CFRP). Therefore, an experimental study investigated the influence of elevated temperatures on the shear behavior of reinforced concrete (RC) beams strengthened externally with CFRP. For this purpose, forty reinforced concrete beams were cast. Thirty-two of them were externally strengthened with CFRP and eight beams were unanchored and left as a control. The beams then were tested under four-point bending to assess their structural performance in terms of failure modes, and load-displacement relations. Results have shown, explicitly, that the control specimens encountered a brittle failure, unlike the ones strengthened with CFRP, as those had a ductile mode. The strengthened beams showed an increase in the ultimate load-carrying capacity accompanied by an enhancement in mid-span deflection in different percentages with respect to the control beam. This technique also improved the shear capacity of the anchorage area, reflecting an improvement in the effectiveness of the anchored CFRP laminates. Finally, the influence of the exposed temperature on the ductility, energy absorption, and ultimate load reduction percentage is significant and increased with the increase of temperature.

1. Introduction

Concrete is the most extensively used material for structures since numerous decades. Nevertheless, concrete material is classified as a brittle material with a low strain limits and tensile strength capacity. There have been ongoing efforts to help overcome these deficiencies using several strategies. The utilization of fibers in structural concrete elements began in 1970s because of their ability in the upgrading the mechanical properties of concrete. These days, broad examinations were completed on the utilization of various types of fibers for enhancing the concrete mechanical properties of structures. Nowadays, carbon fiber-reinforced polymer materials (CFRP) are considered as main strengthening and rehabilitation composite materials of shear or in flexure deficient reinforced concrete structures.

CFRP materials are frequently used in structural engineering applications for repair and strengthening of existing concrete structures. Externally bonded FRP composite is used to strengthen concrete beams in flexure and shear. Many experimental observations indicated that the debonding that occurs at the interface between concrete and FRP is a typical failure mode of reinforced concrete beams strengthened with externally bonded CFRP [1, 2]. CFRP composite materials have come to the forefront as promising materials and systems for structural retrofit. Glass fiber reinforced polymer (GFRP) and carbon fiber reinforced polymer (CFRP) have higher tensile strength but its strength is not fully utilized due to de-bonding problem and brittle tensile behavior. The general influence is clearly an increase in the peak loads of the specimens [3, 4].

Al-Rousan, R. Impact of elevated temperature on the shear behavior of strengthened RC beams. Magazine of Civil Engineering. 2022. 110(2). Article No. 11002. DOI: 10.34910/MCE.110.2

Extreme temperatures harm severely RC structures, including beams, because these structures experience significant degradation in stiffness and strength, in addition to big, consistent deformations [5]. The reason behind this is that high temperatures cause decay in the mechanical properties of concrete and steel rebar, in addition to the stresses' redistribution in the beam [5, 6]. The CFRP sheets are distinguished because they are easy to install, corrosion-resistant, flexible, and ductile. The flexural behavior of RC beams, strengthened with external wraps of CFRP sheets, has been evaluated by several researchers, who found that this technique of strengthening improved the beams' flexural behavior. They, also found that this method helped the heat-damaged elements to restore their flexural strength to an extent. The quality of the heat-damaged beams' recovery or strengthening is governed by a number of factors, such as the material's resistance to fire [5, 7], elevated temperature [8, 9], fiber type [10–13], analysis type [14–18], energy integrity resistance [19], anchored system [20], heating condition [21, 22], the sheets' shape and dimensions, the severity of damage [23], and safety factors for CFRP strengthening of bridges [24].

The concrete's stability in some RC structures (such as chimneys, the area around furnaces, rocket launcher platforms, nuclear power stations, the rabidly extinguished ones) is threatened due to frequent heat cycles heating-cooling cycles resulting from the big gradient in temperatures. Therefore, the design process must consider the heat cycles [5, 25, 26]. In fact, concrete can maintain its mechanical characteristics in temperatures up to 300°C. However, when the concrete is exposed to a temperature exceeding 500 °C, its properties degrade considerably, causing concrete's cracking due to high superficial tensile stresses. In sum, exposing concrete to very high temperatures or big difference in temperatures due to frequent heat cycles or rabid extinguishing of fire lead to a degradation in concrete's integrity because of irregular expansions and contractions of concrete contents, i.e., aggregate and paste of cement. Several factors govern the amount of damage in RC structures, such as the structure's dimensions, type of cement and aggregate, the moisture content in concrete, the duration and how frequent structure is subjected to high temperatures, the cooling method, and the highest obtained temperature [5, 27]. Various methods and materials have been adopted to strengthen and repair concrete structures, such as steel plate bolting, RC jacketing, pre-stressed external tendons, and CFRP laminates. Recently, the CFRP laminates have been used in many applications all over the world because they have many remarkable features, such as: simple to shape and install, high ratio of strength-to-weight, highly strong mechanically, and non-corrosive; as it is worth mentioning that structures are, mostly, endure damages because of: steel's corrosion, heat cycles, and dynamic loads [28-30].

This research is expected to be useful for retrofitting the existing buildings, mainly for buildings located in areas prone to medium earthquake. Therefore, critical concerns to produce a practical and cost-effective material used to retrofit standing concrete buildings [5]. Also, the impact of CFRP external strengthening on the behavior of deficient reinforced concrete beams exposed to elevated temperature must receive miniature consideration. The issue discussed in this study is actually a matter of concern to the practitioners in the field of strengthening and repairing heat-damaged RC beams, particularly that there is very little available literature related to this subject [5]. In this study, experimental program was carried out to find the improvements in the strength and ductility behavior of RC beams confined internally with CFRP. The main parameters studied were number of CFRP strips (1, 2, 3, and 4 strips) and elevated temperature (23 °C, 150 °C, 250 °C, and 500 °C).

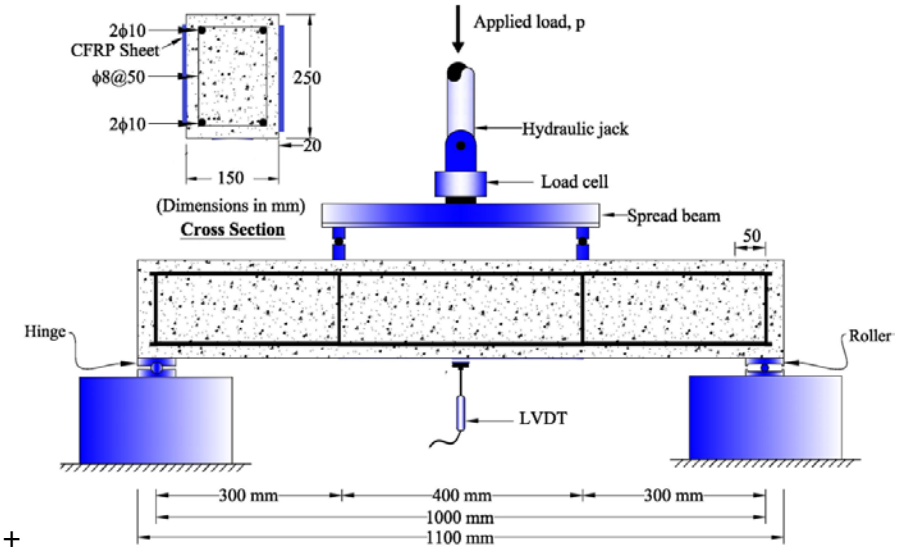

Figure 1. Setup and reinforcement details of the beams.

2. Methods

2.1. Experimental Work

Forty (two beams were made from each type) beams had been constructed and experimented, as simply supported, by subjecting them to four-points loading as shown in Fig. 1. The tested beams were 1100 mm long with cross-sectional dimensions of 150×200 mm. The investigated parameters in this study are the number of CFRP strips (1, 2, 3, and 4 strips) and elevated temperature (23 °C, 150 °C, 250 °C, and 500 °C) as shown in Table 1. The designation and steel reinforcement (yielding stress of 420 MPa) of the tested beams are summarized in Table 1 and Fig. 1, respectively.

Table 1. The details of failure of tested shear beams.

Group	Beam	Temperature, °C	CFRP Configuration	P_u, kN	Δ_u, mm	Steel strain, με	CFRP strain
1	SBT23-0S	23	None	55.7	4.73	0	---
	SBT23-1S		1 Strip of CFRP	59.4	5.27	5040	$0.307\varepsilon_{fu}$
	SBT23-2S		2 Strips of CFRP	63.6	5.55	5318	$0.324\varepsilon_{fu}$
	SBT23-3S		3 Strips of CFRP	68.0	5.99	5624	$0.343\varepsilon_{fu}$
	SBT23-4S		4 Strips of CFRP	72.9	6.16	5878	$0.368\varepsilon_{fu}$
2	SBT150-0S	150	None	52.3	4.49	0	---
	SBT150-1S		1 Strip of CFRP	55.0	4.80	4244	$0.259\varepsilon_{fu}$
	SBT150-2S		2 Strips of CFRP	59.4	5.11	4578	$0.279\varepsilon_{fu}$
	SBT150-3S		3 Strips of CFRP	63.5	5.37	4704	$0.287\varepsilon_{fu}$
	SBT150-4S		4 Strips of CFRP	68.7	5.64	5076	$0.309\varepsilon_{fu}$
3	SBT250-0S	250	None	45.0	4.36	0	---
	SBT250-1S		1 Strip of CFRP	47.4	4.64	4199	$0.256\varepsilon_{fu}$
	SBT250-2S		2 Strips of CFRP	51.7	4.75	4295	$0.262\varepsilon_{fu}$
	SBT250-3S		3 Strips of CFRP	55.1	4.94	4489	$0.274\varepsilon_{fu}$
	SBT250-4S		4 Strips of CFRP	59.3	5.11	4599	$0.280\varepsilon_{fu}$
4	SBT500-0S	500	None	32.9	4.26	0	---
	SBT500-1S		1 Strip of CFRP	34.9	4.39	3513	$0.214\varepsilon_{fu}$
	SBT500-2S		2 Strips of CFRP	38.0	4.53	3732	$0.228\varepsilon_{fu}$
	SBT500-3S		3 Strips of CFRP	40.9	4.79	4044	$0.247\varepsilon_{fu}$
	SBT500-4S		4 Strips of CFRP	43.5	4.99	4204	$0.256\varepsilon_{fu}$

Note: The values between parentheses are normalized with respect to the control, P_u: Ultimate Load, Δ_u: Ultimate deflection, ε_f = CFRP strain, ε_{fu}: CFRP ultimate strain of 16400 με.

2.2. Design of concrete mixture

The mixture of concrete (Table 2) with the proportions by weight of 0.61(water):1.00(cement (Ordinary Type I Portland cement)):2.98(Crushed limestone coarse aggregates with absorption of 2.3 %, a maximum aggregate size of 12.5 mm, and a specific gravity of 2.62)):2.62 (fine aggregates with absorption of 1.9 %, fineness modulus of 2.69, and specific gravity of 2.65). The superplasticizer as a percent of the cement weight was used to improve the workability of the concrete mixture and result a slump of about 50 mm.

Table 2. Mix design proportions.

Ingredient	Quantity (kg/m³)
Cement	269
Water	158
w/c	0.40
Super- plasticizer	8
Coarse aggregate	891
Fine aggregate	834

The beams are casted by using a tilting drum mixer with a capacity of 0.15 m³ (Fig. 2). Firstly, the tilting drum mixer inner surface was wetted. During the tilting drum mixer running, all the crushed limestone coarse aggregates with portion of the used water were added (Fig. 2). After that, the fine aggregates, cement, and water were added gradually. Finally, the super-plasticizer with the last amount of used water was added to the concrete mixture. Lastly, all the concrete mixture ingredients were mixed for five minutes before pouring into wooden molds with inner dimensions of (100×150×1100 mm) and compacted with an electrical vibrator (Fig. 2). After twenty-four hours from the beams casting, all beams were de-molded and then cured in lime-saturated water tank for 28 days (Fig. 2).

Preparing the ingredients of mixture | **Mixing concrete by tilting drum mixer** | **Wooden mold for casting beams**

Casting concrete into molds | **Casting concrete into cylinders** | **Water-cured tank for 28 days**

Figure 2. The mixing, casting, and curing of reinforced concrete beams.

2.3. Heat treatment Method

The average 28-day splitting compressive and tensile strengths of the tested cylinders were 25.0 MPa and 3.0 MPa, respectively. Cylindrical specimens and block were subjected to heat treatment for two hours at temperatures from 150–500 °C before allowed to cool inside the special electrical furnace. The furnace is equipped with an electronic panel to control automatically the time of exposure and the temperature (maximum of 1200 °C). Fig. 3 shows the time-temperature schedule for the furnace.

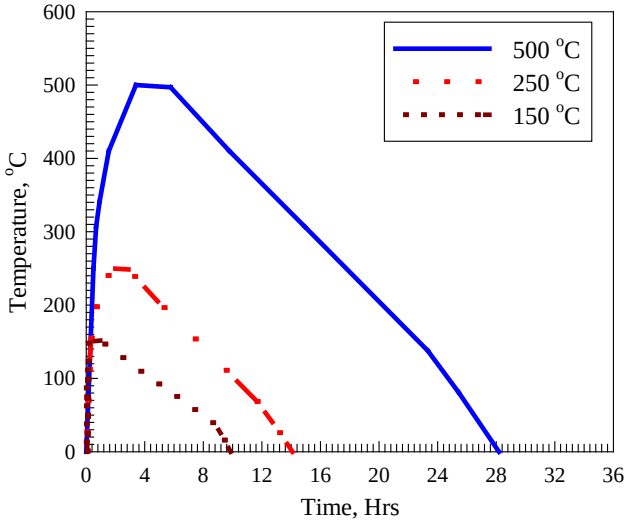

Figure 3. The time-temperature schedule.

The effect of exposing specimens to elevated temperatures is demonstrated in Fig. 4 which depicts the residuals for compressive and slitting strength versus temperature. The curves followed almost similar trend behavior represented in a slight decrease at a temperature of 150 °C followed by a significant decrease at higher temperatures. The detrimental effect of high temperatures greater than 250 °C on both strengths can be referred to thermally induced cracks and/or decomposition of cement binding materials (beyond 250 °C). The damage by heating caused map type cracking which increased with elevated temperature without being accompanied with an apparent surface alteration. The reduction in residual strengths (compressive, splitting) which is (98 %, 97 %) at 150 °C to (61 %, 60 %) at 500 °C, as can be deduced from Fig. 4.

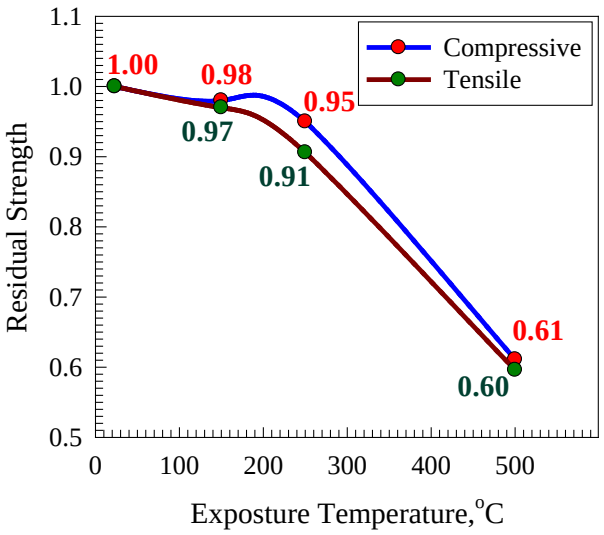

Figure 4. Residuals for compressive and splitting strengths versus exposure temperature.

2.4. Bonding of CFRP sheets to the concrete beams

The concrete beams were demolded after 24 hours of casting and cured in a lime-saturated water tank for 28 days. Firstly, the concrete bonded area were roughened and brushed with steel wire cup brush in order to provide leveled contact between CFRP sheets and concrete (Fig. 5). Secondly, any dust and lose particles was removed from the bonded area by using air vacuum cleaner and then the bonded area was marked while the un-bonded area was covered with plastering tape to be free of epoxy (Fig. 5). Based on investigated parameters, the CFRP composite sheets cut into sheets with a width of 50 mm and different lengths. Thirdly, the epoxy compounds (part A and B) were prepared by using low-speed electric drill for at least 3 minutes to get a homogenous epoxy mixture. Fourthly, the epoxy first layer was applied uniformly over the bonded area and then the CFRP composite sheet (the tensile strength of 4900 MPa, thickness of 0.166 mm, elongation at break of 2.1 %, elastic modulus of 230 GPa) was placed onto the epoxy. Plastic roller was used along the fiber direction in order to remove any entrapped air bubbles. Finally, the epoxy second layer was applied over the CFRP sheet bonded area to make sure epoxy homogeneous distribution (Fig. 5).

Marking the area of CFRP sheets bonded using plastering tape

Concrete bonded area were roughened and brushed with steel wire cup brush

Applying the first layer of epoxy onto CFRP sheets surface

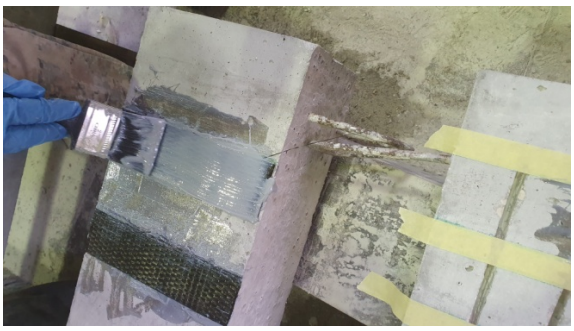

Applying the two layers of epoxy onto CFRP sheets surface

Figure 5. Bonding of CFRP sheets to reinforced concrete beams.

2.5. Testing Setup

All beams were tested under four-point loading with a simply supported span of 1000 mm (Fig. 1). The two supports are one roller and the other one is hinge as well as the loading points were made from steel to make sure zero deformation. A hydraulic testing machine is used to apply the load with a displacement loading rate of 0.1 mm/sec. The vertical linear variable displacement transducer (LVDT) is used to record the mid-span deflection which is placed at the bottom of the beam (Fig. 1). Also, one strain gage was placed in position such that to record the CFRP tensile strain. The tested results (load-deflection curves and the CFRP strain) were collected by using data acquisition system while the failure modes and cracks pattern are obtained visually.

3. Results and Discussion

3.1. Mode of failure

The modes of failure of the control beam as well as the beams with CFRP strips are shown in Fig. 6. All failures were occurred within the shear span as was intentionally designed with inclined failure planes. This allows for a reasonable estimation of the contribution of the CFRP strips to the shear strength of the concrete. Formation of web-shear cracks was observed during loading; the number as well as widths and lengths of the web shear cracks increased as the loading increased. At ultimate, a sudden crushing within the shear span was observed after the development of major multiple web-shear cracks. The loads at which concrete crushing occurred was different reflecting the contribution and effectiveness of the CFRP strips in providing shear resistance. In some occasions, at failure, a significant portion of the concrete shattered from the shear span. Shear failure is sudden in nature and once happens, it causes large inclined cracks accompanied by loud sound. This typically occurs at either one of the beam ends due to very slight variation in the beam or loading after deflection. Compared with the control beam, the shear span of the anchored beams experienced less intense shear cracks with the inner core remained nearly intact. This is attributed to alleviation of the intensity of the web-shear stresses and consequent cracking by the anchored CFRP strips that participated in resisting the induced stresses.

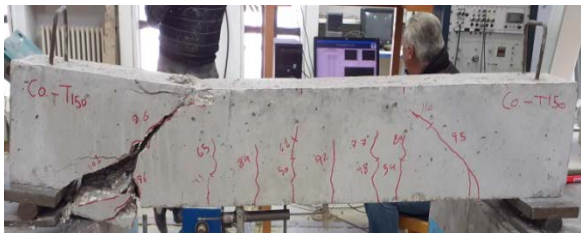

Control

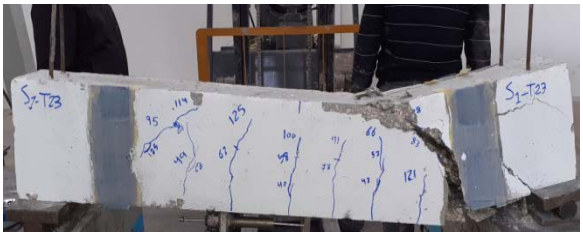

1 CFRP strip

2 CFRP strips

3 CFRP strips **4 CFRP strips**

(a) Effect of number of CFRP strips

23 °C **150 °C**

250 °C **500 °C**

(b) Effect of elevated temperature

Figure 6. Typical mode of failure.

3.2. Strain in CFRP strips

Figure 7 shows the standard curves of load vs. CFRP strain for all the specimens. It could be observed that the emergence of diagonal cracks in concrete produced tensile stresses in CFRP laminates due to the development of shear force. The maximum level of tensile stresses was at the CFRP's middle point, intersecting diagonal cracks, close to the mid-height of the beam's cross-section (Figure 6). Also, the whole specimens' CFRP strain was found to be less than 16400 με, the ultimate value, as illustrated in Table 1. In addition, in Table 1, it was revealed that the number of CFRP strips impacted, to a far extent, the effectiveness of CFRP strips. In strengthened beam specimens at 23 °C, the enhancement percentages, as per the ultimate strain of CFRP strips, were: 30.7 %, 32.4 %, 34.3 %, and 35.8 % for one, two, three, and four strips, respectively, and these percentages are similar to Al-Rousan [5]. At 150 °C, the percentages, as per the ultimate strain of CFRP strips, were: 25.9 %, 27.9 %, 28.7 %, and 30.9 % for one, two, three, and four strips, respectively, achieving 0.85 of the beam's strains at 23ºC, and these percentages are similar to Al-Rousan [5]. At 250 °C, the beams' strain percentages, as per the ultimate strain of CFRP strips, were: 25.6 %, 26.2 %, 27.4 %, and 28.0 % for one, two, three, and four strips, respectively, achieving 0.80 of the beams' strains at 23 °C, and these percentages are similar to Al-Rousan [5]. At 500 °C, the percentages of strains, as per the ultimate strain of CFRP strips, were: 21.4 %, 22.8 %, 24.7 %, and 24.7 % for one, two, three, and four strips respectively, achieving 0.71 of the beams strains at 23 °C.

In the sage of pre-cracking, CFRP strains did not develop. After the emergence of diagonal shear cracks in the shear span, the strains of CFRP became higher, at a fast rate, till failure (Figure 7), and this behavior is similar to Al-Rousan [5]. It was also found that the CFRP's strains CFRP appeared extensively when the bonding area was larger. Results also showed the strain of the CFRP laminates was highly influenced when the specimens were strengthened with four grooved strips of CFRP.

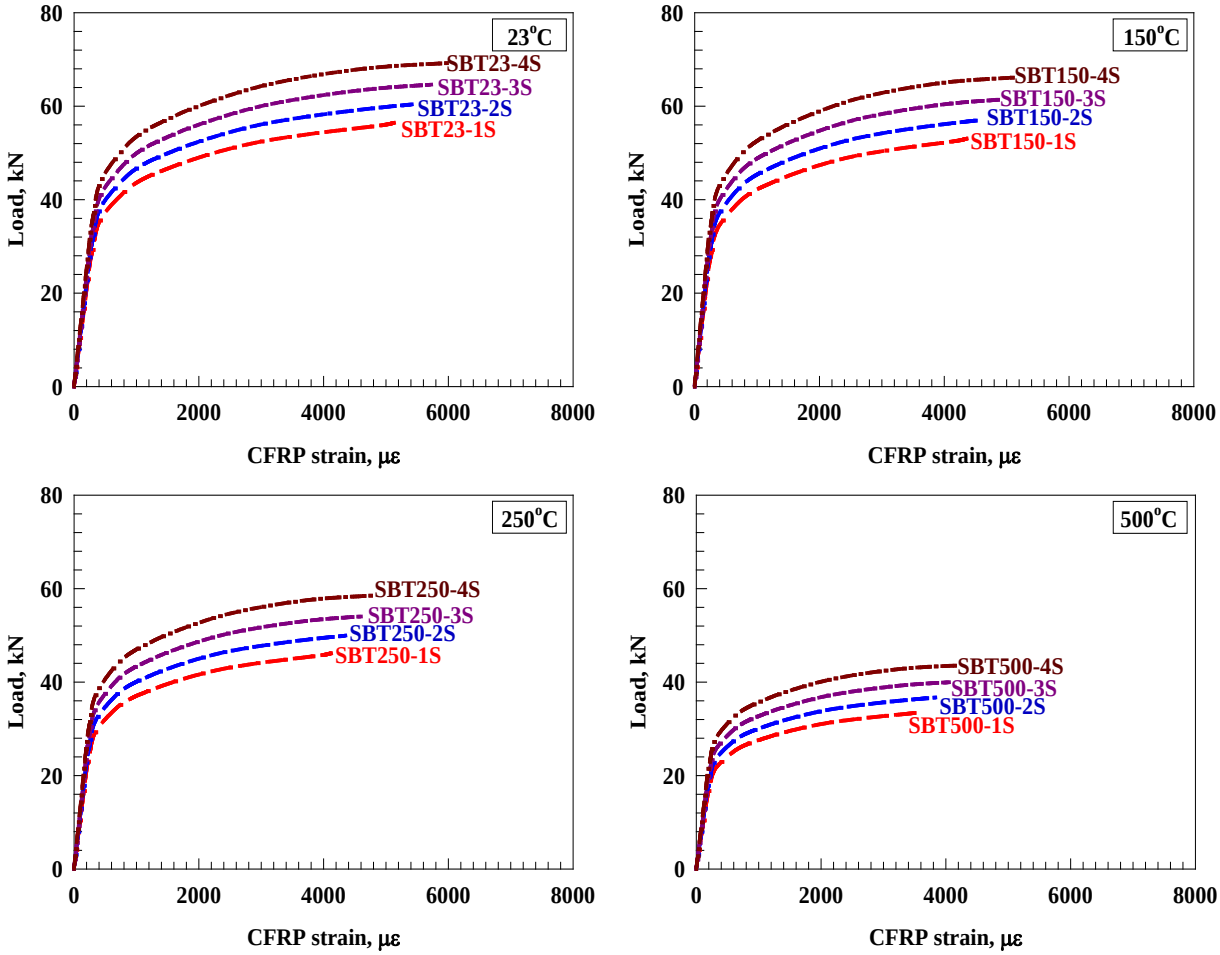

Figure 7. Typical load versus CFRP strain curve

3.3. Load versus deflection behavior

Table 3 shows the load vs. deflection characteristics curves for both anchored and un-anchored strengthened beams and control ones. The characteristics included stiffness and toughness. The initial stiffness can be specified from the slope of the linear elastic stage of the load-deflection curve ($k = P/\delta$) [5]. Also, toughness can be specified by computing the total constrained area underneath the load-deflection curve up to the point of ultimate load capacity [5]. The load vs. deflection, at mid-span, curve (Figure 8) has three distanced parts: the pre-cracking part, it is linearly elastic, and it extends to the first flexural crack; the second part is the transition, extending to the point at which the diagonal shear cracks appear; and the third part is the post-cracking, extending to the beam's ultimate capacity. Inspecting Figure 8, the anchored grooves technique significantly influenced the specimens': toughness, stiffness, ultimate load, and maximum deflection (Table 3). In addition, it has been deduced that the bigger the bonded area of CFRP, the better the beam's behavior. Furthermore, the higher the temperatures, the less the performance (Figure 8).

Table 3. Characteristics of load deflection behavior.

Group	Beam	Temperature, °C	Elastic stiffness (kN/mm)	Toughness (kN.mm^2)	Strength factor	Ductility factor	Performance Factor
1	SBT23-0S	23	13	139	1.00	1.00	1.00
	SBT23-1S		15	186	1.07	1.12	1.19
	SBT23-2S		17	223	1.14	1.17	1.34
	SBT23-3S		19	269	1.22	1.27	1.55
	SBT23-4S		20	301	1.31	1.30	1.71
2	SBT150-0S	150	12	124	0.94	0.95	0.89
	SBT150-1S		14	154	0.99	1.01	1.00
	SBT150-2S		16	190	1.07	1.08	1.15
	SBT150-3S		17	221	1.14	1.14	1.30
	SBT150-4S		19	257	1.23	1.19	1.47

Group	Beam	Temperature, °C	Elastic stiffness (kN/mm)	Toughness (kN.mm^2)	Strength factor	Ductility factor	Performance Factor
3	SBT250-0S	250	11	101	0.81	0.92	0.75
	SBT250-1S		13	126	0.85	0.98	0.83
	SBT250-2S		14	147	0.93	1.00	0.93
	SBT250-3S		16	170	0.99	1.05	1.03
	SBT250-4S		18	194	1.07	1.08	1.15
4	SBT500-0S	500	8	72	0.59	0.90	0.53
	SBT500-1S		9	84	0.63	0.93	0.58
	SBT500-2S		11	101	0.68	0.96	0.65
	SBT500-3S		12	121	0.73	1.01	0.74
	SBT500-4S		13	138	0.78	1.05	0.82

Note: Performance Factor is defined as strength factor multiply by ductility factor

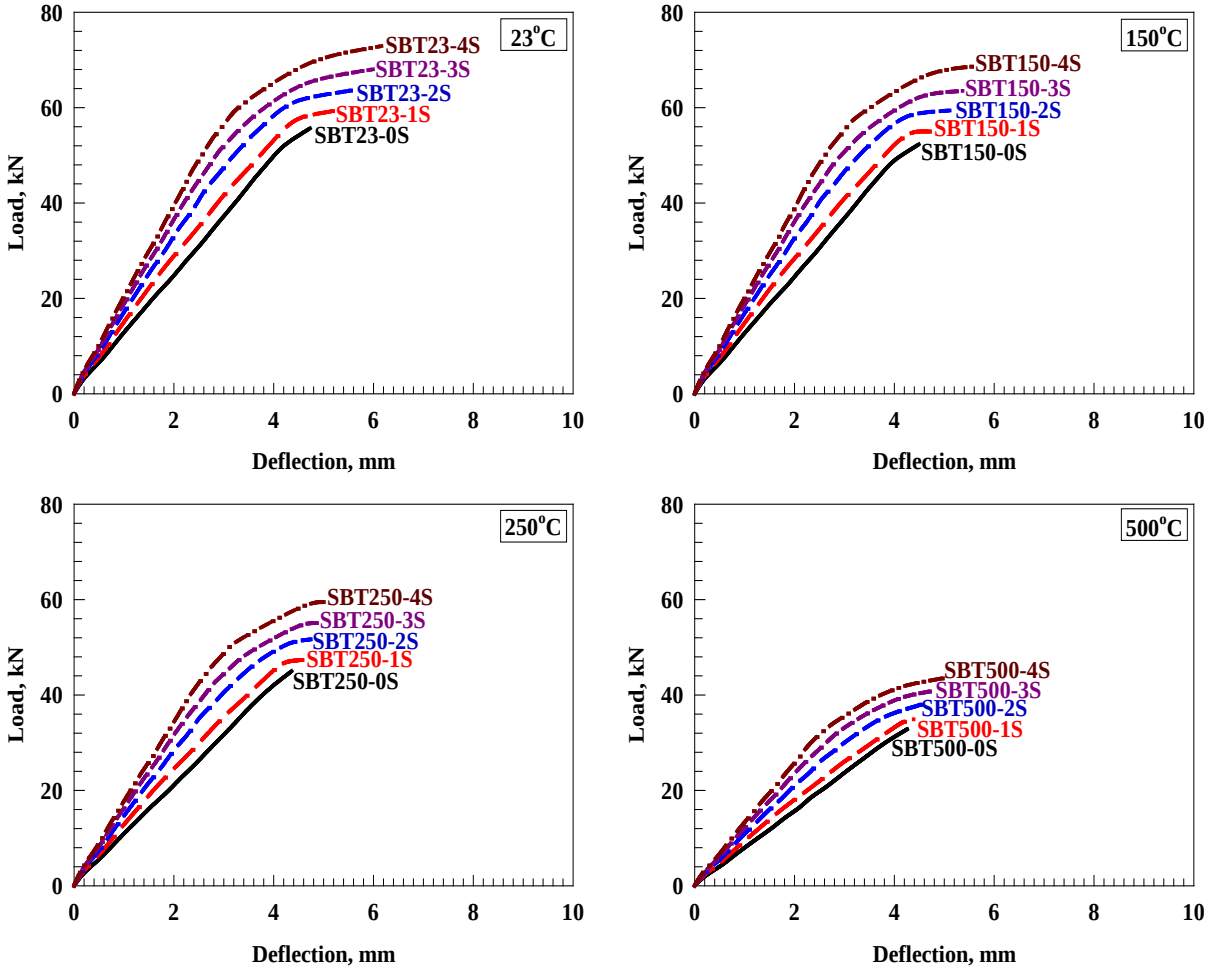

Figure 8. Load-deflection curves for the tested beam.

3.4. Maximum load capacity and corresponding deflection

The evaluation of strengthened RC beams load capacity and resultant deflections has shown tremendous structural performance [5]. The ultimate load capacity is produced by the limit states of the beam's ultimate load, while the deflections are due to the serviceability, as in Table 3. The strengthened beam's load capacity percentage can be found by dividing the ultimate load capacity by the control beam's load capacity [5]. Similarly, the strengthened beam's deflection percentage can be determined by dividing the strengthened beam's ultimate deflection by the control beam's ultimate deflection, as depicted in Figure 9. It is worth mentioning that strength percentage is an indicator of the beam's capability of sustaining load incrementing. Figure 9 showed that rising the number of CFRP strips significantly enhanced the beam's strength percentage. The average ultimate load enhancement percentage (Fig. 9) for tested beams with respect to control beam is 6.7 %, 14.2 %, 22.2 %, and 30.9 % for one, two, three, and four strips, respectively. Whereas, the average ultimate load reduction percentage (Fig. 9) for tested beams with

respect to beams exposed to 23 °C is 6.5 %, 19.1 %, and 40.5 % for 150 °C, 250 °C, and 500 °C strips, respectively.

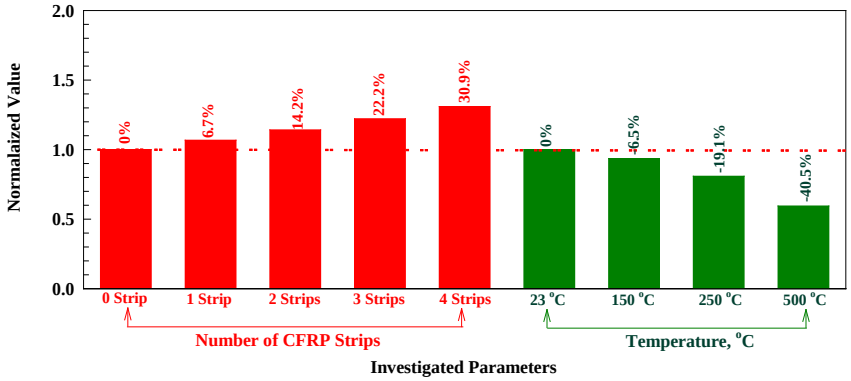

Figure 9. Normalized ultimate load capacity with respect to control beam.

The deflection indicates how much the strengthened RC beams can sustain deformations without failure [5]. The deflection percentage is defined as the ratio of the ultimate deflection of the strengthened beam to the ultimate deflection of the control beam (undamaged beam), as shown in Fig. 10. Fig. 10 shows that the ductility percentage also significantly increased with the increase of the number of CFRP strips and decreased with the increase of exposed temperature. The average ultimate deflection enhancement percentage (Fig. 10) for tested beams with respect to control beam is 6.8 %, 13.7 %, 19.5 %, and 25.6 % for one, two, three, and four strips, respectively, and this equal to 0.83 times the enhancement percentages in ultimate load. Whereas, the average ultimate deflection reduction percentage (Fig. 10) for tested beams with respect to beams exposed to 23 °C is 8.2 %, 13.9 %, and 16.8 % for 150 °C, 250 °C, and 500 °C strips, respectively, and this equal to 0.90 times the reduction percentages in ultimate load.

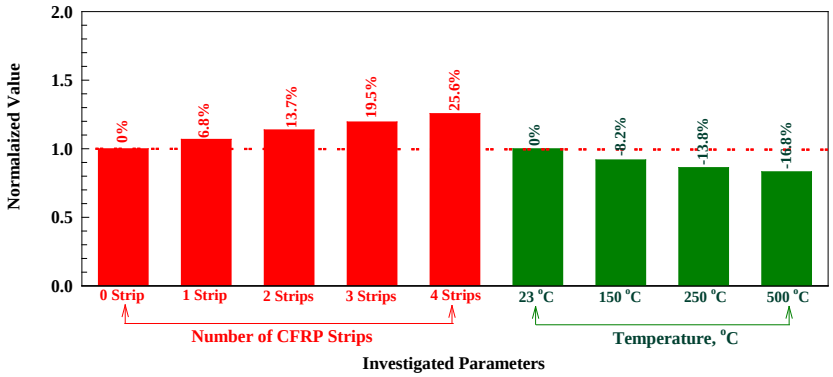

Figure 10. Normalized ultimate deflection with respect to control beam.

3.5. Elastic stiffness

Elastic stiffness indicates the crystal's response to external stresses or strains. Also, stiffness describes the properties of bonding in addition to the stability, mechanically and structurally [5]. The slope of the pre-cracking part of the load-deflection graph represents an elastic stiffness. For the sake of comparison, the values of the CFRP-strengthened specimens' elastic stiffness were modified according to the control beam (Fig. 11).

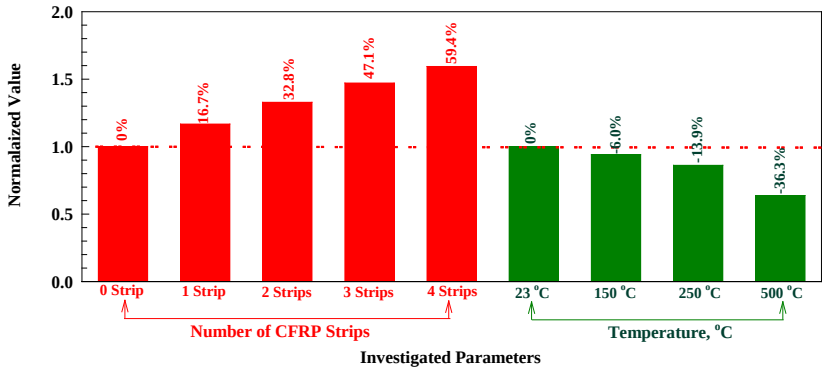

Figure 11. Normalized stiffness with respect to control beam.

In Fig. 11 illustrates the specimens' enhancement percentages of elastic stiffness, as per control beam, averaging 16.7 %, 32.8 %, 47.1 %, and 59.4 % for one, two, three, and four strips, respectively. Whereas, the average elastic stiffness reduction percentage (Figure 11) for tested beams with respect to beams exposed to 23 °C is 6.0 %, 13.9 %, and 36.3 % for 150ºC, 250 °C, and 500 °C strips, respectively.

3.6. Toughness of tested beams

Toughness defines a material's energy absorption capability, per unit volume, before being deformed, plastically, without being ruptured. Toughness can be determined by computing the area beneath the load-deflection curve [5]. The strengthened specimens' toughness values were modified in accordance with the control beams (Fig. 12). Inspection of Fig. 12 reveals that the average toughness enhancement percentage for tested beams with respect to control beam is 33.6 %, 60.7 %, 94.0 %, and 116.9 % for one, two, three, and four strips, respectively. Whereas, the average toughness reduction percentage (Fig. 12) for tested beams with respect to beams exposed to 23 °C is 15 %, 33.3 %, and 53.6 % for 150 °C, 250 °C, and 500 °C strips, respectively.

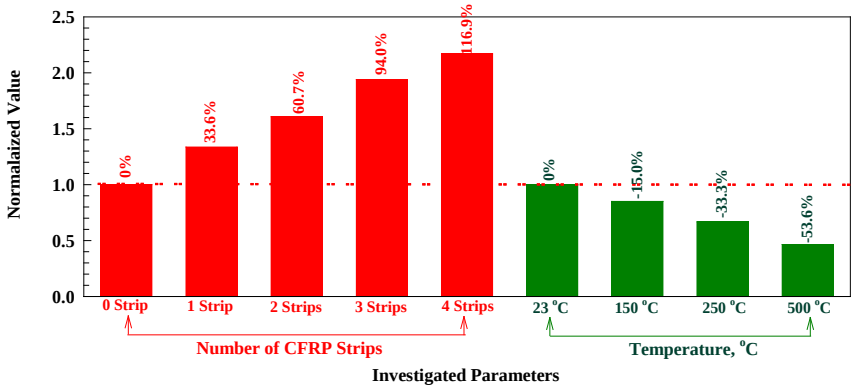

Figure 12. Normalized toughness with respect to control beam.

3.7. Performance evaluation of experimental results

The effectiveness of CFRP laminates was investigated by monitoring three factors: the strength factor (SF), deformability factor (DF), and performance factor (PF), where the PF is SF and DF combined together (Table 3 and Fig. 13) [5]. From Fig. 13, raising the CFRP's bonded area (number of strips) enhanced the PF. On the other side, the PF factor decreased when the temperature was raised. Finally, enlarging the bonded area made the beams highly resistant to the brittle shear failure and enhanced their performance. Inspection of Fig. 13 reveals that the average performance factor enhancement percentage for tested beams with respect to control beam is 55.9 %, 113.4 %, 185.4 %, and 245.7 % for one, two, three, and four strips, respectively. Whereas, the average performance factor reduction percentage (Fig. 13) for tested beams with respect to beams exposed to 23 °C is 20.1 %, 42.6 %, and 70.4 % for 150 °C, 250 °C, and 500 °C strips, respectively.

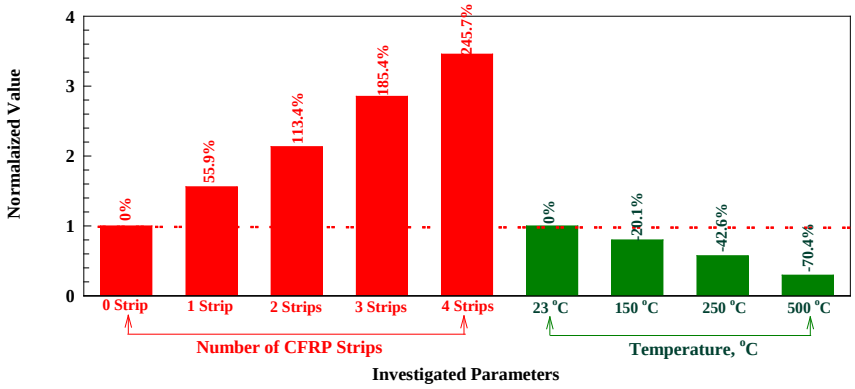

Figure 13. Normalized performance factor with respect to control beam.

Table 4. Index of profitability.

Group Number	Beam	Temperature, °C	Concrete's shear contribution, kN	CFRP shear contribution, kN	Ultimate shear contribution, kN	V_f/A_f, MPa
1	SBT23-0S	23	55.7	0	55.7	0
	SBT23-1S		55.7	3.8	59.4	2.0
	SBT23-2S		55.7	7.9	63.6	1.1
	SBT23-3S		55.7	12.4	68.0	0.8
	SBT23-4S		55.7	17.2	72.9	0.6
2	SBT150-0S	150	52.3	0	52.3	0
	SBT150-1S		52.3	2.7	55.0	1.8
	SBT150-2S		52.3	7.1	59.4	1.0
	SBT150-3S		52.3	11.2	63.5	0.7
	SBT150-4S		52.3	16.4	68.7	0.6
3	SBT250-0S	250	45.0	0	45.0	0
	SBT250-1S		45.0	2.4	47.4	1.6
	SBT250-2S		45.0	6.7	51.7	0.9
	SBT250-3S		45.0	10.1	55.1	0.6
	SBT250-4S		45.0	14.3	59.3	0.5
4	SBT500-0S	500	32.9	0	32.9	0
	SBT500-1S		32.9	2.1	34.9	1.2
	SBT500-2S		32.9	5.1	38.0	0.6
	SBT500-3S		32.9	8.0	40.9	0.5
	SBT500-4S		32.9	10.7	43.5	0.4

Note: V_f: the CFRP shear contribution, A_f : the CFRP bonded area within the shear span

3.8. The index of profitability

For RC beams strengthened with various methods of CFRP, Table 4 illustrates each of the concrete's shear contributions (V_c), the CFRP material's shear contributions (V_f), and the final loads. It was observed that enhancing the bonded area of CFRP (i.e., the number of sheets) increased the contribution of CFRP (V_f) to the shear capacity. A number of strengthening methods, using CFRP laminates, were examined, considering the following aspects: the consumed quantity of CFRP, and the calculated profitability indices. Profitability index is the ratio of CFRP's contribution to shear strength-to-total CFRP bonded area, inside the strengthened beam's shear span with various CFRP methods. Strengthened beams' profitability indices are shown in Table 4, where it is shown that increasing either the number of CFRP sheets (bonded area) or the temperatures has decreased the profitability index.

3.9. Comparison of experimental results with ACI model

For purposes of comparison, the experimental results are compared with ACI model [30], the general design guidance is derived from the experimental data and they are only applicable to external FRP reinforcement. Fig. 14 shows a comparison of the results predicted by the ACI model (V_f, experimental /V_f,ACI [30]). Note that the ACI model was calibrated for CFRP should be used with caution for other types of composites as shown in Fig. 14. The overall predictions by ACI model [30] appear to be overestimated with a mean V_f, experimental /V_f,ACI value of 1.11 and a coefficient of variation (COV) of 26 %. It is also important to take into consideration that all the ACI model are semi empirical in nature, with important governing parameters derived from test data for beams strengthened with FRP laminates, whereas the ACI model cannot be applied in certain cases. In addition, a careful inspection of Fig. 14 will show that the ACI model [30] has a much wider range of experimental/theoretical failure load ratios of 0.80 to 1.46.

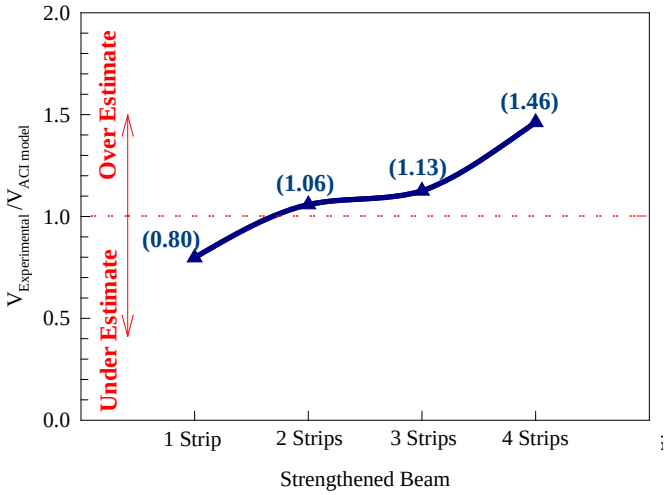

Figure 14. The normalized *e*xperimental FRP shear force with respect to ACI model [41].

4. Conclusions

1. The presence of CFRP strips shifted the forms of end debonding failure modes, i.e. end interfacial debonding and cover separation, to a less critical one, therefore improved the performance of the conventional CFRP-strengthening method.

2. CFRP strips increase the shear capacity of the anchorage zone; therefore result in higher anchorage efficiency of FRP-strengthened concrete beams.

3. The strengthened beams showed an increase in the load-carrying capacity for the strengthened beams accompanied by a reduction in the vertical deflection at the mid-span in different percentages compared with the control beam.

4. The influence of the number of CFRP strips on the ductility, energy absorption, and ultimate load improvement percentage is significant.

5. The influence of the exposed temperature on the ductility, energy absorption, and ultimate load reduction percentage is significant and increased with the increase of temperature.

6. The overall predictions by ACI model [30] appear to be overestimated with a mean value of 1.11 and a coefficient of variation (COV) of 26 %.

5. Acknowledgment

The author gratefully acknowledges the financial support from Deanship of Scientific Research at Jordan University of Science and Technology under Grant number 2021/5.

References

1. Rajai, Z. Al-Rousan. Empirical and NLFEA prediction of bond-slip behavior between DSSF concrete and anchored CFRP composites. Construction and Building Materials. 2018. 169 (1). Pp. 530–542. DOI: 10.1016/j.conbuildmat.2018.03.013
2. Rajai, Z. Al-Rousan. Behavior of macro synthetic fiber concrete beams strengthened with different CFRP composite configurations. Journal of Building Engineering. 2018. 20 (1). Pp. 595–608. DOI: 10.1016/j.jobe.2018.09.009
3. Al-Rousan Rajai, Abo-Msamh Isra'a. Bending and Torsion Behaviour of CFRP Strengthened RC Beams. Magazine of Civil Engineering. 2019. 92 (8). Pp. 62–71. DOI: 10.18720/MCE.92.8
4. Al-Rousan, R. The shear behavior of CFRP Strengthened RC beams. Magazine of Civil Engineering. 2020. No. 6. Pp. 9810–9810. DOI: 10.18720/MCE.98.10
5. Al-Rousan, R. Behavior of strengthened concrete beams damaged by thermal shock. Magazine of Civil Engineering. 2020. No. 2. Pp. 93–107. DOI: 10.18720/MCE.94.8.
6. Al-Rousan, R. Behavior of CFRP strengthened columns damaged by thermal shock. Magazine of Civil Engineering. 2020. No. 5. Pp. 9708–9708. DOI: 10.18720/MCE.97.8
7. Nedviga, E., Beresneva, N., Gravit, M., Blagodatskaya, A. Fire Resistance of Prefabricated Monolithic Reinforced Concrete Slabs of "Marko" Technology. Adv. Intell. Syst. Comput. 2018. 692 (1). Pp. 739–749. DOI: 10.1007/978-3-319-70987-1_78
8. Hezhev, T.A., Zhurtov, A.V., Tsipinov, A.S., Klyuev, S.V. Fire resistant fibre reinforced vermiculite concrete with volcanic application. Magazine of Civil Engineering. 2018. 80 (1). Pp. 181–194. DOI: 10.18720/MCE.80.16
9. Goremikins, V., Blesak, L., Novak, J., Wald, F. Experimental investigation on SFRC behaviour under elevated temperature. Journal of Structural Fire Engineering. 2017. 8 (1). Pp. 287–299. DOI: 10.1108/JSFE-05-2017-0034

10. Goremikins, V., Blesak, L., Novak, J., Wald, F. To testing of steel fibre reinforced concrete at elevated temperature. Applications of Structural Fire Engineering. 2017. 1 (1). Pp. 48–54. DOI: 10.14311/asfe.2015.055
11. Blesak, L., Goremikins, V., Wald, F., Sajdlova, T. Constitutive model of steel fibre reinforced concrete subjected to high temperatures. Acta Polytechnica. 2016. 56 (1). Pp. 417–424. DOI: 10.14311/AP.2016.56.0417
12. Korsun, V., Vatin, N., Franchi, A., Korsun, A., Crespi, P., Mashtaler, S. The strength and strain of high-strength concrete elements with confinement and steel fiber reinforcement including the conditions of the effect of elevated temperatures. Procedia Engineering. 2015. 117 (1). Pp. 970–979. DOI: 10.1016/j.proeng.2015.08.192
13. Goremikins, V., Blesak, L., Novak, J., Wald, F. Experimental method on investigation of fibre reinforced concrete at elevated temperatures. Acta Polytechnica. 2016. 56 (1). Pp. 258–264. DOI: 10.14311/AP.2016.56.0258
14. Selyaev, V.P., Nizina, T.A., Balykov, A.S., Nizin, D.R., Balbalin, A.V. Fractal analysis of deformation curves of fiber-reinforced fine-grained concretes under compression. PNRPU Mechanics Bulletin. 2016. 1 (1). Pp. 129–146. DOI: 10.15593/perm.-mech/2016.1.09
15. Bily, P., Fladr, J., Kohoutkova, A. Finite Element Modelling of a Prestressed Concrete Containment with a Steel Liner. Proceedings of the Fifteenth International Conference on Civil, Structural and Environmental Engineering Computing. Civil-Comp Press. 2015. DOI: 10.4203/ccp.108.1
16. Bílý, P., Kohoutková, A. Sensitivity analysis of numerical model of prestressed concrete containment. Nuclear Engineering and Design. 2015. 295 (1). Pp. 204–214. DOI: 10.1016/j.nucengdes.2015.09.027
17. Al-Rousan, R. Behavior of two-way slabs subjected to drop-weight. Magazine of Civil Engineering. 2019. 90 (6). Pp. 62–71. DOI: 10.18720/MCE.90.6
18. Al-Rousan, R. The impact of cable spacing on the behavior of cable-stayed bridges. Magazine of Civil Engineering. 2019. 91 (7). Pp. 49–59. DOI: 10.18720/MCE.91.5
19. Krishan, A., Rimshin, V., Erofeev, V., Kurbatov, V., Markov, S. The energy integrity resistance to the destruction of the long-term strength concrete. Procedia Engineering. 2015. 117 (1). Pp. 211–217. DOI: 10.1016/j.proeng.2015.08.143
20. Korsun, V., Vatin, N., Korsun, A., Nemova, D. Physical-mechanical properties of the modified fine-grained concrete subjected to thermal effects up to 200°S. Applied Mechanics and Materials. 2014. 633–634. Pp. 1013–1017. DOI: 10.4028/www.scientific.net/AMM.633-634.1013
21. Korsun, V., Korsun, A., Volkov, A. Characteristics of mechanical and rheological properties of concrete under heating conditions up to 200°C. MATEC Web Conference. 2013. 6 (1). Pp. 07002. DOI: 10.1051/matecconf/20130607002
22. Petkova, D., Donchev, T., Wen, J. Experimental study of the performance of CFRP strengthened small scale beams after heating to high temperatures. Construction and Building Materials. 2014. 68 (1). Pp. 55–61. DOI: 10.1016/j.conbuild-mat.2014.06.014
23. Ji, G., Li, G., Alaywan, W. A new fire resistant FRP for externally bonded concrete repair. Construction and Building Materials. 2013. 42 (1). Pp. 87–96. DOI: 10.1016/j.conbuildmat.2013.01.008
24. Trentin, C., Casas, J.R. Safety factors for CFRP strengthening in bending of reinforced concrete bridges. Composite Structures. 2015. 128 (1). Pp. 188–198. DOI: 10.1016/j.compstruct.2015.03.048
25. Ferrari, V.J., de Hanai, J.B., de Souza, R.A. Flexural strengthening of reinforcement concrete beams using high performance fiber reinforcement cement-based composite (HPFRCC) and carbon fiber reinforced polymers (CFRP). Construction and Building Materials. 2013. 48 (1). Pp. 485–498. DOI: 10.1016/j.conbuildmat.2013.07.026
26. Attari, N., Amziane, S., Chemrouk, M. Flexural strengthening of concrete beams using CFRP, GFRP and hybrid FRP sheets. Construction and Building Materials. 2012. 37 (1). Pp. 746– 757. DOI: 10.1016/j.conbuildmat.2012.07.052
27. Kara, I.F., Ashour, A.F., Körog˘lu, M.A. Flexural behavior of hybrid FRP/steel reinforced concrete beams. Composite Structures. 2015. 129 (1). Pp. 111–121. DOI: 10.1016/j.compstruct.2015.03.073
28. Kolchunov, V.I., Dem'yanov, A.I. The modeling method of discrete cracks in reinforced concrete under the torsion with bending. Magazine of Civil Engineering. 2018. 81 (5). Pp. 160–173. DOI: 10.18720/MCE.81.16
29. Travush, V.I., Konin, D.V., Krylov, A.S. Strength of reinforced concrete beams of high-performance concrete and fiber reinforced concrete. Magazine of Civil Engineering. 2018. No. 77 (1). Pp. 90–100. DOI: 10.18720/MCE.77.8
30. ACI Committee 440. Design and Construction of Externally Bonded FRP Systems for strengthening Concrete Structures. *ACI440.2R-02. 2002. American Concrete Institute, Farmington Hills, Mich.: 45 pp. DOI: 10.1061/40753(171)159. ISBN: 9780870312854

Contacts:

Rajai Al-Rousan, rzalrousan@just.edu.jo

Received 12.04.2020. Approved after reviewing 23.12.2020. Accepted 04.03.2021.